Prediction of PDIV in motor coils using finite element method

Stéphane Duchesne, Guillaume Parent, Julien Moeneclaey, Daniel Roger

Prediction of PDIV in Motor Coils Using Finite Elements Method

Stéphane Duchesne, Guillaume Parent, Julien Moenecley and Daniel Roger
Univ. Artois,EA 4025, Laboratoire Systèmes Électrotechniques et Environnement, (LSEE)
F-62400, Béthune, France
Email: http://www.lsee.fr

***Abstract*—The aim of this paper is the presentation of a method allowing the prediction, at the design phase, of the partial discharges Inception Voltage (PDIV) in motor coils made with classical enamelled wire. The method is based on the comparison of electrical potential values — obtain with a Finite elements simulation — with those given by the Paschen's laws for the same inter-electrode gap. The originality of the study is the consideration of the length of the electric field lines to compute the gap between the electrodes. With this prediction, it is possible to improve the capabilities of the Electrical Insulation System (EIS) of motor built in large series.**

I. Introduction

Last few years have seen the development of more and more electric vehicles. The embedded power growth lied to use the electrical activators with very strong environmental or electrical constraints. For example, with more than 1,4MW of embedded power, the *Dreamliner* is the most electric aircraft for the moment and many systems are targeted to produce a new generation of planes like braking, de-icing systems, taxiing, passengers equipments, air conditioning and pressuring. These embedded systems have to deal with the weight of the copper conductors, and thus, the trend tries to increase the value of the supply voltage, much higher than usual voltage. Moreover, the enamelled wires technology uses a classical combination of polyamide-imide (PAI) and polyester-imide (PEI) — whose thickness are defined in an international standard [1] — designed for industrial voltages operating points. In addition, the motors are currently fed by PWM converters without any filter due to weight considerations. In these conditions, the steep voltage edges imposed to the system made of the motor and the connection cable causes a voltage peak that may exceed the partial discharges inception voltage (PDIV) in the motor insulation system [2]. When they appear, partial discharges (PD) cause very fast ageing of polymer insulating layers leading to a short life expectancy for standard motors fed by these systems [3], [4]. The variable operating conditions of the embedded systems can lead to unconventional values of the PDIV. Indeed, the conditions of appearance of partial discharges are intrinsically linked to pressure, temperature or humidity. So, it is necessary to calculate a relevant value of this threshold very early during the design of the motor to adjust its EIS. The method used in this study suggests to compute the distribution of the electric field in a motor coil to compare the results with those calculated with the Paschen's theory. In a first part, the method is detailed and validated with the suitable assumptions. Then, the use of the method in the domain of the coil insulation is explained. Geometrical and environmental consideration are took into account to refine the results quality. The third part, presents two ways for the method usage, on one hand, for the determination of the PDIV, and on the other hand, for the localisation of the critical area where the PD can appear. The examples are presented on twisted pairs. The last part discusses the results and the ways of improvement for the study.

II. Detail of the Method

A. Paschen's theory

The Paschen's law is given by eq. (1a) and (1b), it allows the determination of the disruptive voltage level responsible for discharge apparition in gases.

$$V_{Breakdown} = \frac{B.p \times d}{C + ln(p \times d)} \tag{1a}$$

$$C = ln\left(\frac{A}{1 + ln\left(\frac{1}{\gamma}\right)}\right) \tag{1b}$$

where A and B depend on the gases characteristics and γ is called *Townsend* secondary emission coefficient. These expressions are obtained experimentally with planar electrodes without insulation. With the parameters given in Table I — for air — the variation of the breakdown voltage with the pressure p or the distance between the electrodes d can be computed. Fig. 1 shows these variations with respect to the product $p \times d$ given in $\mathrm{Torr} \cdot \mathrm{cm}$.

Below the blue curve, the conditions of pressure, distance or voltage do not allow the apparition of discharge (nodes A and B for example). Above that curve, discharges can appear in case of presence of a free electron to initiate the avalanche breakdown process (node C). In that case the Paschen's law does not give a precise criteria of disruptive level but a strong probability of breakdown tied to the probability of presence of

TABLE I: Typical parameters for Paschen law in air [5]

Notation	Value	Unity
A	15	$[\mathrm{Torr}^{-1} \cdot \mathrm{cm}^{-1}]$
B	306	[V]
γ	0.01	[-]

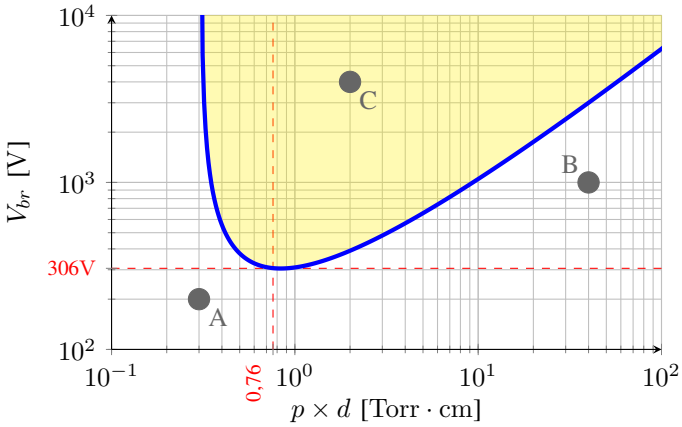

Fig. 1: Paschen law

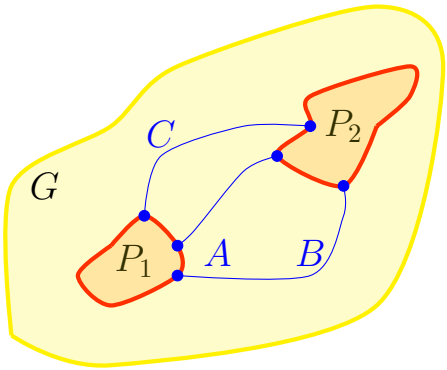

Fig. 2: Field lines occuring between two objects

a seed electron. With such rules — derived from measurements made with planar electrodes — the electric field is uniform.

B. Paschen's law for determination of discharge precursors

According to the Paschen's law, we have to determine, for a given gas and for a given geometry, the value of the electric field and the length of the field lines. Fig. 2 presents a theoretical case of two objects O_1 and O_2 with different potential voltage value along their boundary (in red) which are placed in a gas G (in yellow) under constant pressure conditions. A set of electric field lines can be drawn between the two objects. These lines follow the tangential direction of the electric field produces by the electric charges of the objects. Consequently, it is possible to make the assumption that the electrons presents in this space follow the field lines. For an electrostatic case, the forces occurring the electrons are the gravity and the electrostatic force. The latter being way much higher, the gravity can be neglected. Considering this point, the smooth curve of the field lines and the limited variations of the field values along the line, we can apply locally, the Paschen's law.

Knowing each field line location, it is possible to compute its length and thanks to the potential difference between its two extremities, we are able to place a node corresponding to the considered field line in the plan ($p \times d$,V_{br}) defined in Fig. 1 for a given pressure value. Fig. 2 presents three field lines (A,B and C) which correspond, for example, to the three points plotted in Fig. 1. By computing the whole set of field lines surrounding the two objects, it is possible to determine the smaller value of the breakdown voltage for a given system. In addition, we are, also, able to know the critical position of the field line allowing discharges apparition.

C. Condition of discharges appearance with Finite elements method

We can compute Maxwell's equations 2a, 2b and 2c to obtain the distribution of the electric field intensity $\mathbf{E}$ and the electric flux density $\mathbf{D}$ in a given domain.

$$\boldsymbol{\nabla} \cdot \mathbf{D} = \rho \tag{2a}$$

$$\boldsymbol{\nabla} \times \mathbf{E} = \mathbf{0} \tag{2b}$$

$$\mathbf{D} = \epsilon \mathbf{E} \tag{2c}$$

There are 2 ways to solve these equations. The most commonly used calculate thanks to the scalar potential formulation which solve eq. 3 where v is the electric scalar potential [6]. This method — called $\mathbf{E}$-oriented — is the fastest and the cheapest from the numerical standpoint. Unfortunately, this formulation does not allow the computation of the field lines.

$$\mathbf{E} = -\boldsymbol{\nabla} v \tag{3}$$

A second approach used the dual formulation using the electric vector potential u. This $\mathbf{D}$-oriented method solve eq. 4 [7]. This formulation is rarely used due to a more difficult implementation. Indeed, since $\boldsymbol{\nabla} \cdot \mathbf{D} \neq \mathbf{0}$ the computation of the vector potential u is not straightforward.

$$\mathbf{D} = \boldsymbol{\nabla} \times \mathbf{u} \tag{4}$$

By computing the $\mathbf{D}$-oriented formulation in a 2 dimensional domain, the vector potential u have a single component in a direction normal to the whole domain — a scalar component. So, by definition, the iso-values of u_z draw the electric field lines and the calculation of the vector potential allows the computation of the field line length.

By computing the problem twice — first time with the $\mathbf{E}$-oriented formulation and second time with the $\mathbf{D}$-oriented formulation — the whole needed informations are available. We can drawn a scatterplot given by the previous calculations and make a comparison with the Paschen curve to determine the possibility of discharge appearance.

III. Application of the method to EIS

The application of the suggested method on a classical motor Electrical Insulation System (EIS) need to make some assumptions and to take into account the specificity of the problem.

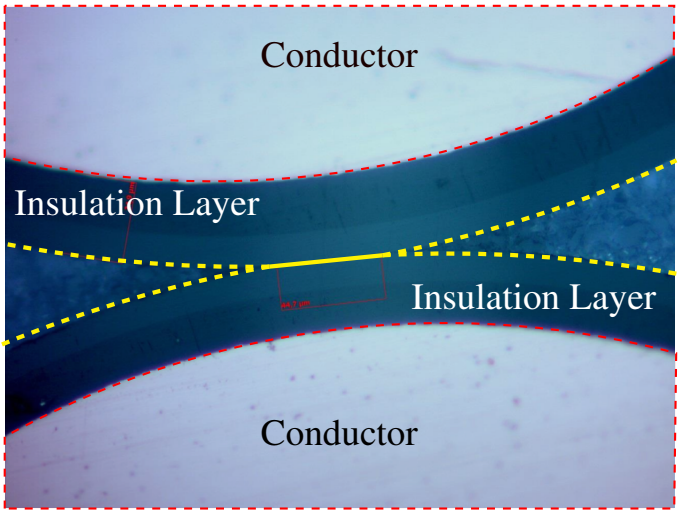

Fig. 3: Wires details

TABLE II: Environmental conditions

Temperature	21.2	°C
Pressure	1013	hPa
Humidity	30	%
Elevation	26	m
Wire Diameter	0.71	mm
Insulation Thickness	44	µm
Length of the contact zone	32	µm
Relative permittivity of insulation	2.7	-

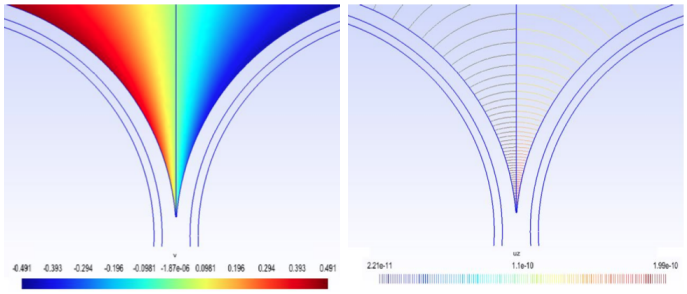

(a) Potential distribution in V (b) Electric field lines

Fig. 4: Results of the finite elements simulation

A. Inclusion of insulations layers

First of all, the presence of insulation layers around the electrodes leads to a particular discharge rate in which there are partial. Indeed, with a dielectric barrier, the discharges are extinguished naturally due to the charge accumulation on the insulation layers boundaries. Many studies showed that the insulation layers have no significant influence on the *Townsend* avalanche mechanism and so on the conditions of appearance of the discharges [8], [9]. The insulation impacts more strongly the discharge extinction conditions. In our case, we can assume that the Paschen's laws gives the threshold voltage allowing partial discharges appearance which is called partial discharges Inception Voltage (PDIV).

B. Geometric considerations

We have to take into account the particularity of the geometry of each studied case to have more precise results. The geometrical considerations influence, obviously, the finite elements model, but also the *Paschen* theory via the secondary emission coefficient of *Townsend* γ.

1) Geometry of the problem: The vicinity area between two wires has to be finely modeled. The thickness of the insulation layer and the gap between the wires have values in the same order of magnitude that the *Paschen* minimum — 306 volt for 100µm gap at atmospheric pressure. Slight variation of the geometry of this area have a strong influence on the calculated PDIV. Thanks to the microscopy presented at Fig. 3 — the different materials are underline — we can see that in the heart of a coil, with the imposed filling factor, the wires are very tight and a planar contact zone appears between two wires.

2) Influence of γ: The secondary emission coefficient of *Townsend* γ represents the number of free electrons issued from the cathode for each impact of a positive ion. This coefficient depends on many parameters like the gas density, the energy acquired by the ions during the impact and, also, the electrodes shapes and material. The secondary emission phenomena allows the self-fuelling of the discharge with the injection of new electrons in the gas. The values of γ are known, or well estimated for the conductor materials, however, for polymers, like the insulation layers of a classical enamelled wire, these values are less well-known [10].

IV. Results

A. Conditions during measurement

In order to obtain the more precise results we have to record the environmental conditions during each measurement. These parameters — summarized at the Table II — will allow to use the most suitable *Paschen* curve. The Table II gives also, the geometrical parameters of the tested wire. In this conditions a set of measurement shows a value of PDIV equal to 935V with a confident interval of 23V.

B. Determination of PDIV

Fig. 4 presents the two solutions obtained with our finite elements model. The first simulation gives the map of the Fig. 4a where the distribution of the electrical potential distribution is drawn. The second simulation gives the electric field lines which are plotted at the Fig. 4b. It is important to note that whole phenomenon are linear, therefore, we can compute the FE simulation per unit.

For this kind of problem, the length of the field lines are steadily increasing and thus, it is possible to plot the red curve of the Fig. 5. This curve represents the variations of the potential difference following the field lines length. By adding a curve representing the critical level of PD appearance computed with Paschen's laws — in green at the Fig. 5— we are able to determine the PDIV. The *Paschen* curve has to take into account the environmental condition measured during the tests. Many tools are available to consider the variations of

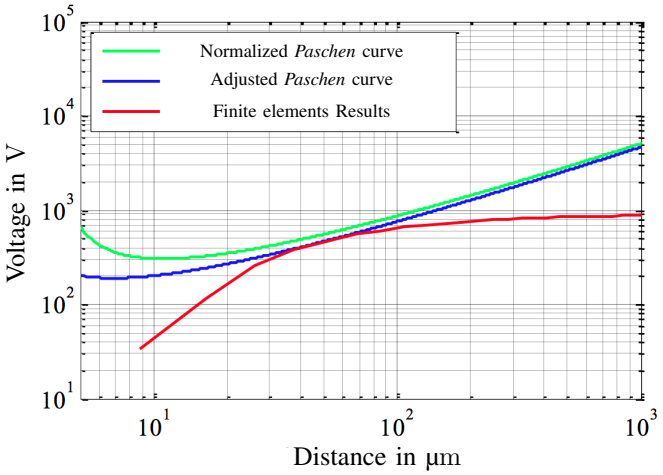

Fig. 5: Determination of PDIV

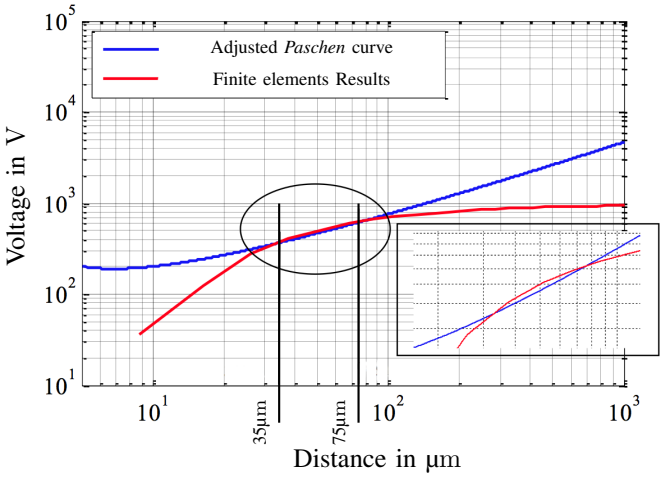

Fig. 6: Localisation of partial dischargess critical area

temperature, pressure [11], [12] or humidity [13]. That allows to add a *Paschen* curve — in blue — at the Fig. 5. We have to tangent the red and blue curve thanks to a multiplicative factor applied on the Finite elements Results to obtain the PDIV value which is equal to the previous factor. In comparison with the measurement, the simulation gives a PDIV value equal to 946 V which remains in the measurement confident interval.

C. Localisation of partial discharges

The presented method, can be used to localise the area within which the appearance of partial discharges is expected in determinate electrical and environmental conditions. By using the value of the supply voltage to shift the finite elements curve the intersection with the *Paschen* curve will define the critical area — wherever the finite elements curve is above the *Paschen* one. In the presented example, a voltage of 1000 V is applied — which is 5% higher than PDIV — and the critical area is located between two electric field lines whose length is between 35 and 75 µm.

V. Discussion

It is possible to refine the accuracy of the method thanks to a better definition of the different parameters used in Paschen's laws. In particular the secondary emission coefficient γ need to be well known for the polymers materials. By computing two Finite elements simulations the results depend strongly of the mesh quality, and this method is not totally rigorous. A better way would calculate the whole informations with one simulation. Some theoretical difficulties impede this, however, works are in progress to allow an easiest and a more precise simulation. The results presented in this study are carried out on twisted pair built with standard enamelled wires. The application to a motor coil need to know the turn to turn maximum voltage between each wires. That is possible thanks to simulation made with equivalent circuits of the whole coil [14]. With the maximum voltages between each wire, by using a microscopy of the coil to adjust the geometry, it is possible to determine the PDIV of the coil, and then, the location of the weaker point of the coil.

VI. Conclusion

The study presented in this paper shows a method allowing the determination of the PDIV on a elementary EIS built with a twisted pair. The general assumptions used for the establishment of the work are presented, discuss and justified. The context of the EIS is, then, approached. An example computed on a standardized twisted pair shows the accuracy of the calculus, and secondly, a localisation of critical area for a given voltage is shown. In a last part, the results are discuss. Ways to improve the determination of the PDIV are proposed and the principle to simply extend the method to a motor coil thanks to previous works.

Acknowledgment

This work is supported by program MEDEE supervised by MEDEE (Maitrise Énergetique Des Entraênements Electriques). This program, including SAFRAN, is sponsored by the Nord-Pas de Calais Region (France) and the European funds (FEDER).

References

[1] *CEI 60317-0-1 : Spcifications pour types particuliers de fils de bobinage*, CEI Std., 2008.

[2] H. Okubo, Y. Lu, M. Morikawa, and N. Hayakawa, "Partial discharge inception characteristics influenced by stressed wire length of inverter-fed motor," in *Electrical Insulation and Dielectric Phenomena, 2004. CEIDP'04. 2004 Annual Report Conference on*. IEEE, 2004, pp. 442–445.

[3] D. Fabiani, G. Montanari, and A. Contin, "Aging acceleration of insulating materials for electrical machine windings supplied by pwm in the presence and in the absence of partial discharges," in *Solid Dielectrics, 2001. ICSD'01. Proceedings of the 2001 IEEE 7th International Conference on*. IEEE, 2001, pp. 283–286.

[4] M. Kaufhold, G. Borner, M. Eberhardt, and J. Speck, "Failure mechanism of the interturn insulation of low voltage electric machines fed by pulse-controlled inverters," *Electrical insulation magazine, IEEE*, vol. 12, no. 5, pp. 9–16, 1996.

[5] T. Dakin, G. Luxa, G. Opperman, J. Vigreux, G. Wind, and H. Winkel, "Phénomènes disruptifs dans un gaz en champ uniforme. courbe de paschen pour lazote, lair et lhexafluorure de soufre," *Electra*, vol. 32, pp. 62–82, 1974.

[6] R. P. Feynman, R. B. Leighton, and M. Sands, *The Feynman lectures on physics, vol. 2: Mainly electromagnetism and matter*. Addison-Wesley, 1979.

[7] Z. Ren, "A 3d vector potential formulation using edge element for electrostatic field computation," *Magnetics, IEEE Transactions on*, vol. 31, no. 3, pp. 1520–1523, 1995.

[8] M. Beyer, W. Boeck, K. Möller, and W. Zaengl, *Hochspannungstechnik: theoretische und praktische Grundlagen*. Springer-Verlag, 2013.

[9] E. Sili, "Etude et caractérisation des décharges partielles et du vieillissement du polyimide en environnement aéronautique," Ph.D. dissertation, Université de Toulouse, Université Toulouse III-Paul Sabatier, 2012.

[10] A. Shih, J. Yater, C. Hor, and R. Abrams, "Secondary electron emission studies," *Applied surface science*, vol. 111, pp. 251–258, 1997.

[11] W. Dunbar *et al.*, "High voltage design criteria," *Nasa-CR-149341 (Boeing Co., Seattle, Wash.), Test and Evaluation Branch Electro-Mechanical Division Astrionics Laboratory*, 1972.

[12] F. W. Peek, *Dielectric phenomena in high voltage engineering*. McGraw-Hill Book Company, Incorporated, 1920.

[13] P. Mikropoulos, C. Stassinopoulos, and B. Sarigiannidou, "Positive streamer propagation and breakdown in air: the influence of humidity," *Dielectrics and Electrical Insulation, IEEE Transactions on*, vol. 15, no. 2, pp. 416–425, 2008.

[14] V. Mihaila, S. Duchesne, and D. Roger, "A simulation method to predict the turn-to-turn voltage spikes in a pwm fed motor winding," *IEEE Transactions on Dielectrics and Electrical Insulation (DEIS)*, vol. 18, no. 5, pp. 1609–1615, 2011.